

Antibacterial activity of chitosan and zinc oxide impregnated in PVA-based membranes

Atividade antibacteriana de membranas de PVA impregnadas com quitosana e óxido de zinco

Actividad antibacteriana de membranas de PVA impregnadas con quitosano y óxido de zinc

Received: 02/24/2023 | Revised: 03/09/2023 | Accepted: 03/10/2023 | Published: 03/14/2023

Edmo Henrique Martins Cavalcante

ORCID: <https://orcid.org/0000-0003-0509-4475>
Universidade Federal Rural de Pernambuco, Brasil
E-mail: edmo-uni@outlook.com

Fernando Antônio Gomes da Silva Junior

ORCID: <https://orcid.org/0000-0003-4096-8828>
Universidade Federal do Vale do São Francisco, Brasil
E-mail: nando.if@hotmail.com

Monica Aparecida Tomé Pereira

ORCID: <https://orcid.org/0000-0001-6565-6762>
Universidade Federal do Vale do São Francisco, Brasil
E-mail: monica.tome@univasf.edu.br

Paulo José Pereira

ORCID: <https://orcid.org/0000-0002-4436-8304>
Universidade Federal do Vale do São Francisco, Brasil
E-mail: paulo.pereira@univasf.edu.br

Mateus MatiuZZi da Costa

ORCID: <https://orcid.org/0000-0002-9884-2112>
Universidade Federal do Vale do São Francisco, Brasil
E-mail: mateus.costa@univasf.edu.br

Helinando Pequeno de Oliveira

ORCID: <https://orcid.org/0000-0002-7565-5576>
Universidade Federal do Vale do São Francisco, Brasil
E-mail: helinando.oliveira@univasf.edu.br

Abstract

The development of alternatives to conventional antibiotics against superbugs represents an important step to avoid the increasing resistance of bacteria observed in conventional treatments. Herein, it was evaluated the influence of different combinations of two active antibacterial components (chitosan and zinc oxide) and a host poly (vinyl alcohol - PVA) in membranes produced by the solvent casting technique. Those systems were evaluated in terms of the biofilm inactivation, kill-time assays and inhibition haloes against *S. aureus* (ATCC 25923) in membranes that must release reactive components while preserving their integrity and favoring the generation of reactive species to improve the antibacterial activity. The results suggest the potential of the combination of chitosan, zinc oxide and poly (vinyl alcohol) to inhibit the growth of *S. aureus* colonies since the PVA improved the dispersion of the components, whereas chitosan-ZnO chelate improves the mutual activity of the metal oxide and the natural polymer template.

Keywords: Membranes; Biomaterials; Surfaces and interfaces; Blends.

Resumo

O desenvolvimento de alternativas aos antibióticos convencionais contra superbactérias representa um passo importante para evitar o aumento da resistência das bactérias diante dos tratamentos convencionais. Neste trabalho, avaliou-se a influência de diferentes combinações de dois componentes antibacterianos ativos (quitosana e óxido de zinco) e uma matriz de álcool polivinílico (PVA) em membranas produzidas pela técnica de evaporação de solvente. Esses sistemas foram avaliados em termos de inativação do biofilme, ensaios de tempo de morte e halos de inibição contra *S. aureus* (ATCC 25923) em membranas que devem liberar componentes reativos, preservando a integridade do material e favorecendo a geração de espécies reativas para melhorar a atividade antibacteriana. Os resultados sugerem o potencial da combinação de quitosana, óxido de zinco e álcool polivinílico para inibir o crescimento de *S. aureus*, uma vez que o PVA melhorou a dispersão dos componentes, enquanto o quelato de quitosana-ZnO melhora a atividade mútua do óxido metálico e do polímero natural.

Palavras-chave: Membranas; Biomateriais; Superfícies e interfaces; Misturas.

Resumen

El desarrollo de alternativas a los antibióticos convencionales contra las superbacterias representa un paso importante para evitar la creciente resistencia de las bacterias observada en los tratamientos convencionales. En esta invención, se evaluó la influencia de diferentes combinaciones de dos componentes antibacterianos activos (quitosano y óxido de zinc) y una base de alcohol polivinílico (PVA) en membranas producidas por la técnica de evaporación de disolvente. Estos sistemas se evaluaron en términos de inactivación de biopelículas, ensayos de tiempo de muerte y halos de inhibición contra *S. aureus* (ATCC 25923) en membranas que deben liberar componentes reactivos preservando su integridad y favoreciendo la generación de especies reactivas para mejorar la actividad antibacteriana. Los resultados sugieren el potencial de la combinación de quitosano, óxido de zinc y alcohol polivinílico para inhibir el crecimiento de *S. aureus*, ya que el PVA mejoró la dispersión de los componentes, mientras que el quelato de quitosano-ZnO mejora la actividad mutua del óxido metálico y el polímero natural.

Palabras clave: Membranas; Biomateriales; Superficies e interfaces; Mezclas.

1. Introduction

The resistance of bacteria against antibiotics has been considered one of the most important challenges to global human health (Kadiyala et al., 2018), since it is observed through a diversity of mechanisms, such as the expression under degradation, modification, or inactivation of antibiotics (Godoy-Gallardo et al., 2021; Niño-Martínez et al., 2019). Skin and soft tissues are the most common parts of the body affected by bacterial infections, which can reach since smallest extent until severe conditions (Burnham & Kollef, 2018). *Staphylococcus aureus* is one of the most common infectious agents (Brandt et al., 2018) while biofilms have been considered the most critical source of failure in antibacterial therapy (particularly in skin wounds) (Bhattacharya et al., 2015; Wang et al., 2018).

The use of nanomaterials represents a new and promising strategy for the development of alternative antibacterial agents to conventional antibiotics (Djurišić et al., 2015). The bactericidal and bacteriostatic effects of several nanomaterials have been reported in the literature, as observed from experimental systems based on Ag₂O, CuO, MgO, TiO₂ and ZnO nanoparticles (Dadi et al., 2019; Dharmaraj et al., 2021; Hajizadeh et al., 2020; Maji et al., 2020).

The surface and morphology-based properties of these materials affect the reactivity in response to high pores density and surface area of materials with the production of reactive oxygen species (ROS), as a result of the partial reduction of oxygen (Soren et al., 2018). For example, superoxide anion (O₂⁻), hydrogen peroxide (H₂O₂) and hydroxyl radical (HO•) can induce damage to the bacterial cell envelope by lipid peroxidation, leading to the intracellular leakage of the content and subsequent death of the microorganism (Singh et al., 2019). These ROS can be efficiently transported to the aqueous medium, provoking the death of bacteria (Milionis et al., 2020).

Amongst metal oxide nanoparticles, zinc oxide has been considered a material with cytocompatibility and antibacterial behavior that presents selective toxicity to prokaryotic cells in comparison to eukaryotes (Dharmaraj et al., 2021; Jiang et al., 2018). Reddy et al. (2007) reported that human cells are considerably more resistant to ZnO nanoparticles toxicity than *Escherichia coli* and *Staphylococcus aureus*, suggesting that these materials are useful as selective therapeutic dosing regimens. In addition to the prevailing hypothesis of ROS production, it is reported the actuation of different mechanisms in zinc oxide that are attributed to their toxicity in prokaryotes. Zn²⁺ ions have intrinsic antimicrobial properties due to the specificity of certain proteins to cofactors such as zinc, which, at toxic levels, can bind to the polypeptide chain, damaging functional groups such as amine, hydroxyl, and sulfhydryl (Lemire et al., 2013; Qi et al., 2017). At a high concentration in the extracellular medium, this compound can also induce competitive inhibition in the assimilation of other metal ions, inhibiting the growth of bacterial cells (McDevitt et al., 2011). The therapeutic window of zinc oxide is reported to be dependent on the preparation method. Disposed of nanoparticles, the antibacterial effectiveness is established at low concentrations (0.16–5.00 mmol/L) (Gudkov et al., 2021). For samples prepared by the wet chemical method, it is reported values in the order of 0.1 to 0.4 g/mL against *E. coli* on MHA medium (Souza et al., 2019) while for samples produced by the sol-gel method, concentrations in the order of 0.5 mg/mL were tested against *B. subtilis*, *E. coli* and *C. albicans* (Khan et al., 2016).

Kadiyala et al. (2018) reported cytotoxicity mechanisms through the analysis of gene expression in methicillin-resistant *S. aureus* in response to ZnO nanoparticles. The authors identified a lower expression of amino acid synthesis and a higher expression of sugar degradation. This observation reinforces nanoparticles' biomimetic mode of action that can be similar in size, shape and charge to certain globular proteins (Kotov, 2010).

On the other hand, chitosan is a linear polymer consisting of N-acetylglucosamine and glucosamine monomers joined by β -(1–4) glycosidic bonds, observed in fungi (Mucoraceae) (Xia et al., 2020). Due to its low toxicity, biodegradability and antibacterial properties, chitosan and its derivatives have been considered promising systems for different applications (Moeini et al., 2020).

In particular, the strong bacterial inhibitory activity of chitosan is observed in acidic media, in which chitosan is soluble with a positive liquid charge net (Sahariah et al., 2014). The advantages of chitosan over other types of biocides are its strong antibacterial activity, the broad spectrum of action and the lower toxicity against mammalian cells (Bhattacharjee et al., 2021). Chitosan can alter cellular permeability by blocking nutrient flow and provoke the disruption of the membrane of microorganisms (Inbaraj et al., 2020), acting as a chelating agent that can bind to traces of dispersed metals in the cytoplasm, inhibiting toxin production and microbial growth (Cuero et al., 1991). In addition, chitosan interacts with the microbial nucleoid and inhibits mRNA synthesis, with direct consequences on protein synthesis (Ma et al., 2017).

In addition, it is worth mentioning that chitosan plays a significant role in the controlled release of active components and the chemical stability of the therapeutic agents as the core is surrounded by a chitosan shell (Raza et al., 2020). However, chitosan has drawbacks such as mechanical weakness, low stability in acid medium, and resistance to mass transfer, which are circumvented by physical and chemical approaches observed by incorporation of materials in different supports such as membranes, beads, and sponges, including metal incorporation, cross-linking and grafting (Ayub et al., 2020) that are useful in tailoring the swelling capacity of the chitosan (Ayub & Raza, 2021).

Besides the chitosan, poly (vinyl alcohol) (PVA) has been considered as a host for the incorporation of metal oxide particles to obtain desirable features such as tensile strength, thermal stability, hydrophilic nature and minimum aggregation. The PVA chain has an abundance of hydroxyl groups that can make hydrogen bonds with oxide in a wide range of composites (Aslam, Kalyar, et al., 2021; Mushtaq et al., 2022). For example, ZnO-loaded PVA nanocomposite films have enhanced tensile strength and Young's moduli (Aslam et al., 2018). These composites, combined with natural materials (e.g. chitosan), offer a route to integrate the characteristics of components (Aslam, Raza, et al., 2021). Solvent casting, electrospinning, gas foaming, and melt modeling are conventional techniques applied in the fabrication of PVA scaffolds applied in the biomedical field (Aslam et al., 2018, 2019).

Under the association of zinc oxide and chitosan, the controlled release of Zn²⁺ can be achieved by coating chitosan nanoparticles with ZnO (Barreto et al., 2017). The bonding between Zn ions with the amines and hydroxyl groups of chitosan can generate free electron donors, improving the biological activity of the chitosan-ZnO compound (Krishnaveni & Thambidurai, 2013). The biocidal activity of these complexes against *S. aureus* has been attributed to the loss of bacterial cell integrity, the release of ions and oxidative stress (Ahmad Yusof et al., 2019; Karthikeyan et al., 2020; Li et al., 2010).

Poly(vinyl alcohol) (PVA) has been considered in different biomedical applications, such as wound dressing and drug delivery, due to its biological advantages such as nontoxicity, noncarcinogenicity, biodegradability, and bioadhesiveness (Fahmy et al., 2015). The combination of PVA and natural/ synthetic polymers confers advantages such as hydration and controlled release of antiseptics (Kamoun et al., 2015). Furthermore, the ZnO powder can be incorporated into PVA to obtain the desired characteristics of wound dressings, such as absorbing the wound fluids and exudates, as well as improving mechanical stability and flexibility (Khalilipour & Paydayesh, 2019).

Herein, it is introduced the novelty of an alternative system of membranes composed of combinations of PVA, zinc oxide and chitosan as a part of a strategy to reach the adequate activity of membranes against *S. aureus*. The objective of this work is focused on the optimization of the combination of components to reach the more effective antibacterial activity of nanocomposites. With this aim, experiments of inhibition haloes, kill-time kinetic assays and biofilm inhibition were performed to evaluate the efficiency of different experimental systems as antibacterial agents, which were explored from different combinations of components to reach an optimized response in terms of the kinetics of bacterial kill-time and the inhibition in the biofilm formation.

2. Methodology

2.1 Materials

Chitosan polymer (C₆H₁₁NO₄)_n of low molecular weight (175.16 g.mol⁻¹) and deacetylation degree of 93% (Exodus Científica, Brazil), poly(vinyl alcohol) – PVA (C₂H₄O)_n, with a degree of hydrolysis of 86.5% - 89.0% and average molecular weight of 30,000-70,000 (MH3 Industrial, Brazil), and zinc oxide (ZnO) with purity higher than 99.0% (Sigma-Aldrich, USA) were used as received. The solutions were prepared in Milli Q® ultrapure water (resistivity of 18.2 MΩ.cm⁻¹) and P.A. acetic acid (CH₃COOH) (Vetec, Brazil).

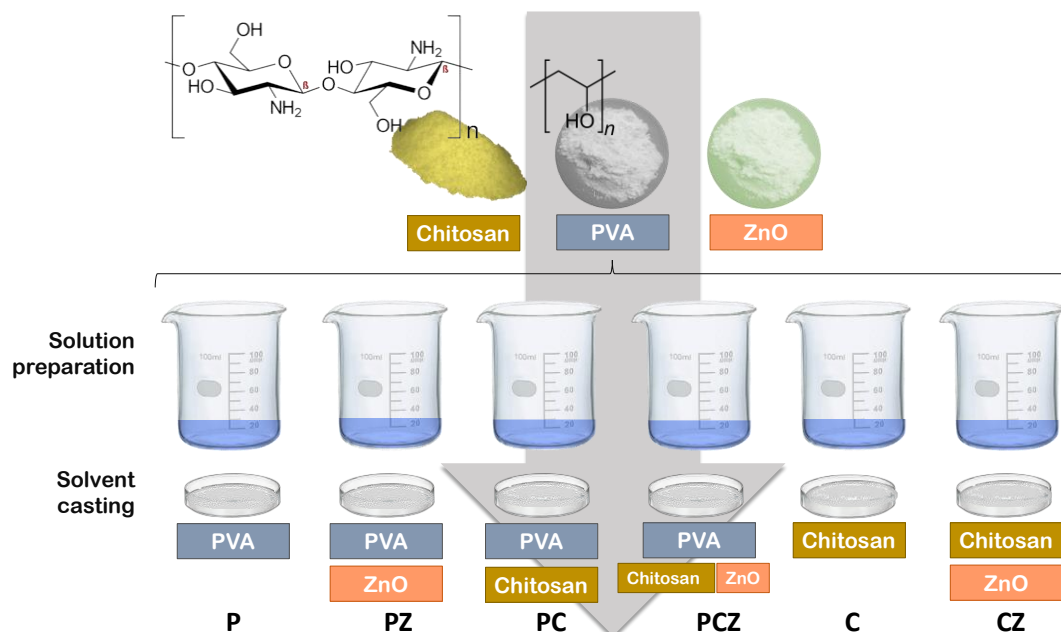
2.2 Membranes preparation

The standard methodology for the production of nanocomposites based on conventional polymers and metal oxides has been reported in the literature (Abdeen et al., 2018; Abureesh et al., 2018; Ahmad Yusof et al., 2019). Modifications in the general procedures were provided in a complete group of quantitative experiments, described as follows: six different types of membranes were prepared, described as follows: the pure PVA membrane (sample P) was prepared from the dispersion of PVA (0.10 g mL⁻¹) in 20 mL of water at 95 °C for 1 h. The membrane of PVA and ZnO (PZ sample) was prepared under the same concentration of the pure PVA (0.10 g mL⁻¹), with the previous dispersion of 0.5% w/v of the metal oxide at corresponding experimental conditions for sample P.

The preparation of the membrane of PVA with chitosan (PC sample) was established as follows: PVA (0.10 g mL⁻¹) was initially dispersed in water (10 mL) at 95°C for 1 h. After that, the temperature of the solution was reduced to 60 °C and a corresponding volume of 1% acetic acid in 10 mL was added to the initial solution. As a following step, 1% w/v of chitosan was added and the solution was stirred for an additional 1 h. The membrane with three components (PCZ sample) was prepared with the dispersion of 0.5% w/v of ZnO after the addition of the acetic acid solution to the PVA solution with the chitosan incorporated after the complete dispersion of the oxide at corresponding conditions for the preparation of sample CZ.

The chitosan membrane (sample C) was prepared with the dispersion of 2% w/v (20 mL) of the biopolymer in 1% acetic acid. The resulting system was stirred at 60 °C for 1 h. The membrane of zinc oxide and chitosan (CZ sample) was prepared by adding 0.5% w/v of ZnO into the 1% acetic acid solution (20 mL). After its complete dispersion, 2 % w/v of chitosan was added, and the solution was kept under stirring for 1 h at 60 °C. The resulting solution was placed in a Petri dish and allowed to evaporate the solvent at room temperature for 48 h. The overall process of membranes preparation is summarized in Figure 1 which is represented the structure of components, the process of preparation of solutions, the solvent casting in Petri dishes for the following evaporation of the solvent and the removal of the solid membrane (P, PZ, PC, PCZ, C and CZ).

Figure 1 - Schematic representation of the overall process of membranes preparation by solvent casting method, considering the combination of components (PVA, chitosan and ZnO). The steps of preparation are followed by the evaporation of the solvent that provides the adequate formation of the solid films.



Source: Authors.

2.3 Characterization

All scanning electron microscopy images were obtained using a scanning electron microscope, Vega 3XM Tescan model equipment (Brno-Kohoutovice, Czech Republic) with an accelerating voltage of 20 kV that were explored to evaluate the morphology of the membranes. The FTIR spectrum was obtained to scrutinize the molecular structures using the KBr method in a Prestige-21 Fourier Shimadzu IR model equipment (Kyoto, Japan) and confirm the structure of the building blocks of the membrane. For the quantification of crystal violet-stained biofilms, the Hach DR5000 spectrophotometer (Manassas, VA, USA) was used, which recorded the spectrum of stained biofilm in the range between 200 nm and 800 nm, in steps of 1 nm. These data are relevant since it represents a direct estimation of the relative concentration of remaining biofilm after treatment.

2.4 Inhibition halo assays

The bacterial inoculum of *S. aureus* (ATCC 25923) was prepared from a culture maintained in agar at 4 °C with a bacterial solution with a concentration of 108 CFU mL⁻¹ homogeneously distributed with a swab on a Petri dish containing Mueller Hinton Agar. Five disk-shaped membranes of 0.8 cm in diameter were carefully deposited on agar for each sample. The plates were placed in an incubator for 24 h at 37 °C. The relevance of the components on the overall inhibition of bacterial growth was evaluated from the inhibition halo values provided by the membranes which were applied as an input for the analysis of variance (one-way ANOVA), with five replicates. This analysis aims to identify the statistical significance of at least one of the parameters, with a confidence of 95% ($\alpha=5\%$).

2.5 Biofilm formation assays

Using a bacteriological loop, *S. aureus* inoculum (ATCC 25923) was dispersed in 20 mL of Tryptic Soy Broth (TSB) in five test tubes. After preparing the bacterial solutions, membranes of PZ, PC, PCZ, CZ, and C were added to each tube. A

sixth tube containing the bacterial solution was used as a negative control sample. The six tubes were then incubated at 37 °C for 24 h.

After this process, the quantification of the relative biofilm formation in the tubes was performed and bacterial solutions were discarded with the tubes washed with ultrapure water. After that, the tubes were kept in contact with the crystal violet solution (1%) for 3 min to stain the grown biofilms. Subsequently, the solutions were discarded, and the tubes were washed with water to remove residues of dye. Finally, an alcohol-acetone solution was prepared to remove the dye stained in the biofilms. The quantification of biofilms was determined by ultraviolet-visible (UV-vis) spectroscopy from the measurement of the absorbance of the solutions at 570 nm (characteristic peak of the dye).

2.6 Time kill kinetics assay

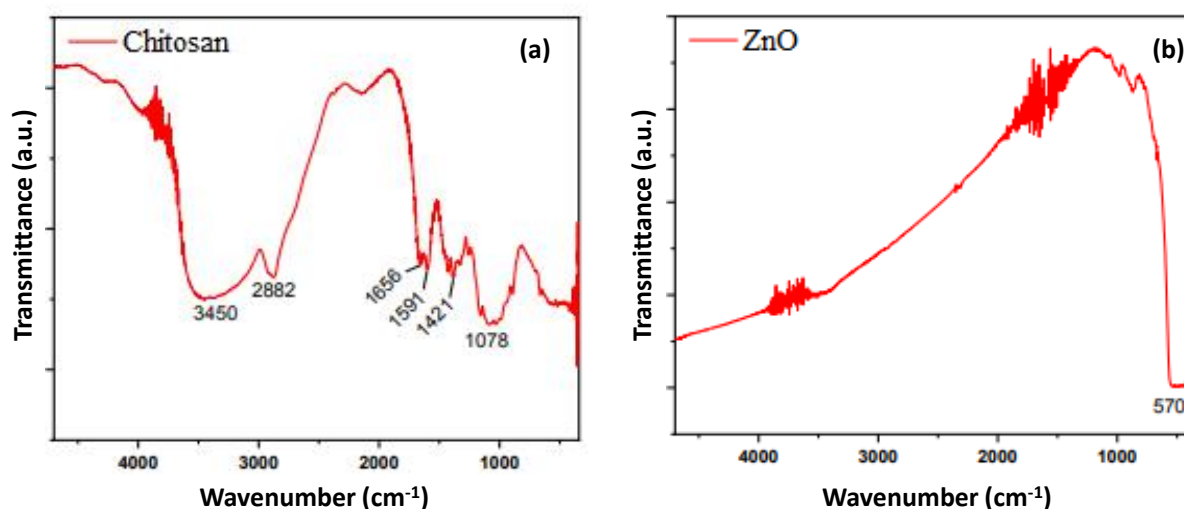
The determination of the kinetics of the death of bacteria by their interaction with different membranes was conducted as follows: 106 CFU mL⁻¹ of bacterial solutions were prepared and disposed of in five test tubes. The samples (PZ, PC, PCZ, CZ, and C) were added to their respective tubes and kept under stirring. Aliquots of 100 µL from each tube were removed at a specific time interval (from 15 min to 420 min) and placed in Petri dishes containing culture medium and incubated at 37 °C for 24 h. After that process, the viable colonies were counted, and the triplicate of each experimental group was considered to average the dynamics of viable bacterial cell reduction.

3. Results and Discussions

3.1 FTIR spectroscopic analysis of components

The structure of additives incorporated in the PVA matrix was examined by the FTIR spectrum shown in Figures 2a and 2b for chitosan and zinc oxide, respectively. The characteristic functional groups in chitosan are shown in Figure 2a in which a broad absorption band between 3500 and 3300 cm⁻¹ is observed, associated with stretching of the primary amine (NH₂) and the hydroxyl groups (OH) (Delgadillo-Armendariz et al., 2014).

Figure 2 - FTIR spectrum of components of antibacterial membranes: (a) chitosan, (b) ZnO, with the indication of the characteristic bands that confirm the natures of explored materials. The identification of compounds scrutinized in the spectra is highlighted by values incorporated in the bands.



Source: Authors.

The absorption bands in 2925 and 2882 cm^{-1} in Figure 2a are assigned to symmetric and asymmetric stretching in the groups CH_2 in the biopolymer (Feng & Peng, 2012). The spectrum also presents characteristic bands in 1656 and 1078 cm^{-1} assigned to the $\text{C}=\text{O}$ axial deformation in the primary amide and the $\text{C}-\text{O}$ stretching, respectively (Gavalayan, 2016). The absorption signal near 1591 cm^{-1} is assigned to the $\text{N}-\text{H}$ deformation of the primary and secondary amine groups (Bobu et al., 2011).

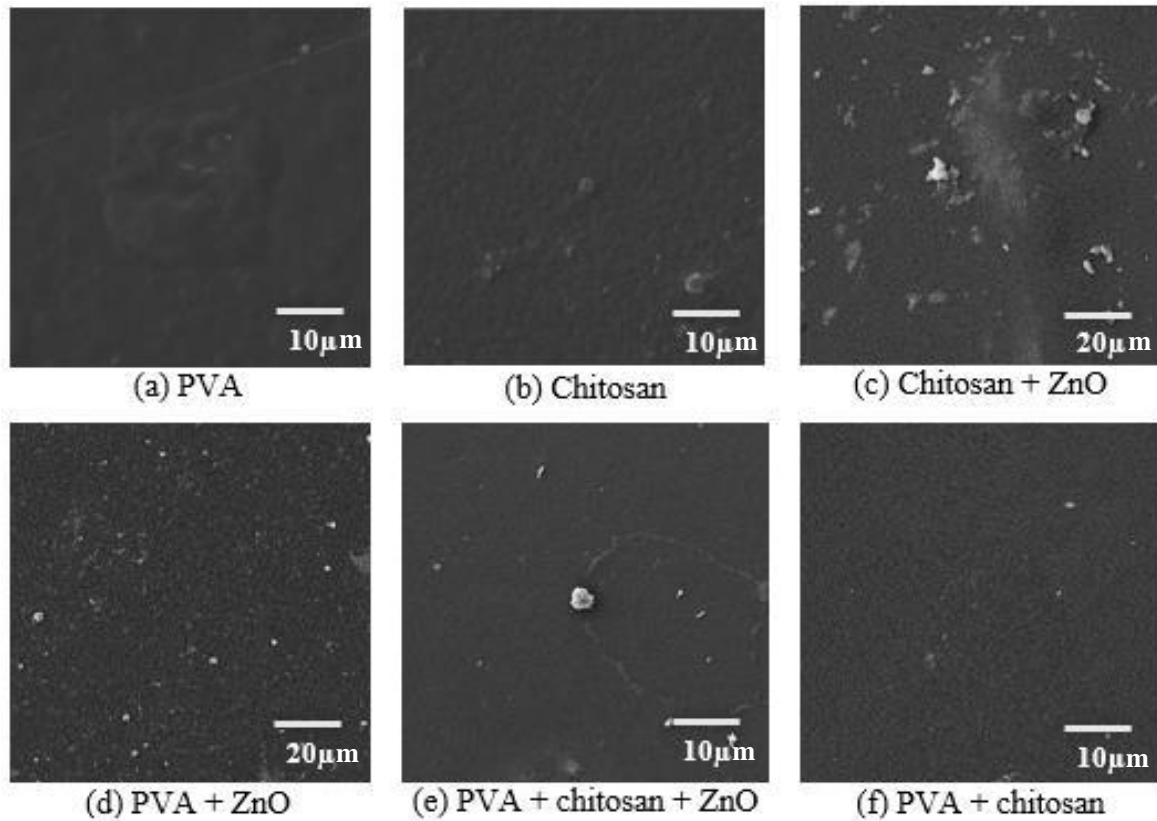
Furthermore, absorption is also perceived in 1421 cm^{-1} , which is a characteristic sign of angular depletion of CH_2 and CH_3 (Paul et al., 2014). The bands associated with $\text{Zn}-\text{O}$ stretching vibration are visualized in 570 cm^{-1} (see Figure 2b) which are assigned to the characteristic ZnO signature (Kajbafvala et al., 2010).

3.2 Morphology of membranes

The morphology of membranes was evaluated by scanning electron microscopies. As shown in Figure 3a, homogeneous distribution of PVA on film is observed for the sample with pure PVA with a corresponding structure for chitosan film in which scarce grains are observed on its surface, indicating the good dispersion of material (see Figure 3b). In agreement with these findings, the presence of scarce grains of additives is also observed for samples prepared with the dispersion of zinc oxide in chitosan (Figure 3c), zinc oxide in PVA (Figure 3d), chitosan and zinc oxide in the PVA substrate (Figure 3e) and chitosan blended into PVA (Figure 3f).

The presence of grains of various sizes in SEM image for sample chitosan + ZnO (Figure 3c) is due to the high molecular weight of chitosan that leads to bridge flocculation, in which the chains are adsorbed for different amounts of particles (Nasu & Otsubo, 2006). In addition, the low density of aggregates on the surface of membranes represents an important aspect of the homogeneous dispersion of antibacterial agents in the membrane, allowing a high density of available sites for bacterial capture and killing can be established.

Figure 3 - SEM images of surface membranes prepared with different combination of additives: (a) pure PVA (3 kx); (b) chitosan (3 kx); (c) chitosan+ZnO (1 kx); (d) PVA+ZnO (1 kx); (e) PVA+chitosan+ZnO (3 kx) and (f) PVA+chitosan (3 kx). The good dispersion of components on the surface of solid films is a general characteristic of the homogeneous dispersion of additives.

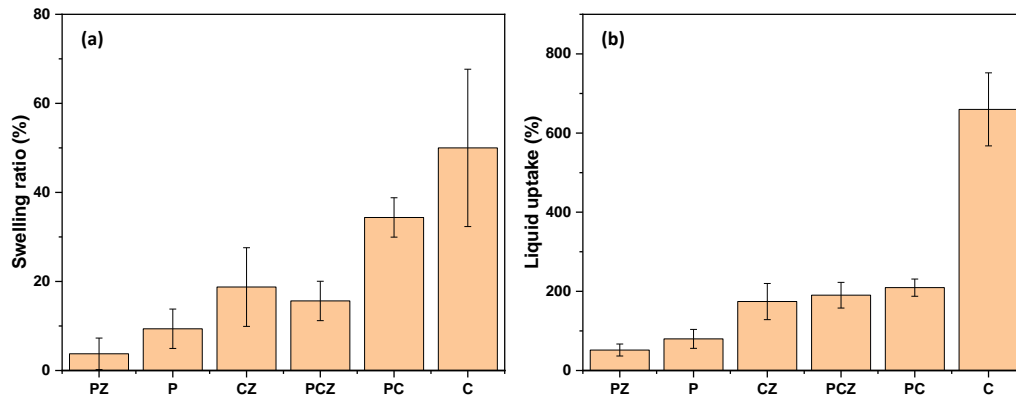


Source: Authors.

Other important parameters to be considered for membranes are the swelling ratio (measured from the relative variation in the diameter of disks after 24 h of immersion of membranes in culture media) and the liquid uptake (defined as the variation in the mass of membranes after 24 h of immersion in the culture media and the mass of the as-prepared membrane (dry condition)) since these parameters return valuable information about the permeability of membranes to liquids. As shown in Figure 4a (for the swelling ratio of the prepared membranes) the higher values are observed for samples prepared with chitosan, confirming the intrinsic property of the chitosan-based membranes to absorb liquids.

On the other hand, the incorporation of PVA reduces the characteristic values for swelling ratio with the lowest value observed for sample PZ. The same behavior is observed for liquid uptake in membranes (see Figure 4b) with a strong variation in the mass of chitosan-based membranes and a reduction in this value for mutual incorporation of PVA and ZnO. These results indicate that high diffusion of components is favored by membranes that incorporate the chitosan while the combined action of PVA and ZnO with chitosan returns lower values for both swelling ratio and liquid uptake, as a result from competition established between the retention provided by PVA and the expansion of the chitosan-based compounds. The limited variation in the swelling ratio and liquid uptake offered by the combination of PVA and ZnO-based samples introduces advantages relative to the retention in the antibacterial activity of components (prolonged and continuous action against *S. aureus*).

Figure 4 - (a) Comparison of the swelling ratio of culture media (MHA) in different membranes (P, PZ, PC, PCZ, C and CZ) and (b) comparison of liquid uptake (MHA) in different membranes (P, PZ, PC, PCZ, C and CZ), confirming the high degree of swelling and liquid uptake for pure chitosan systems.



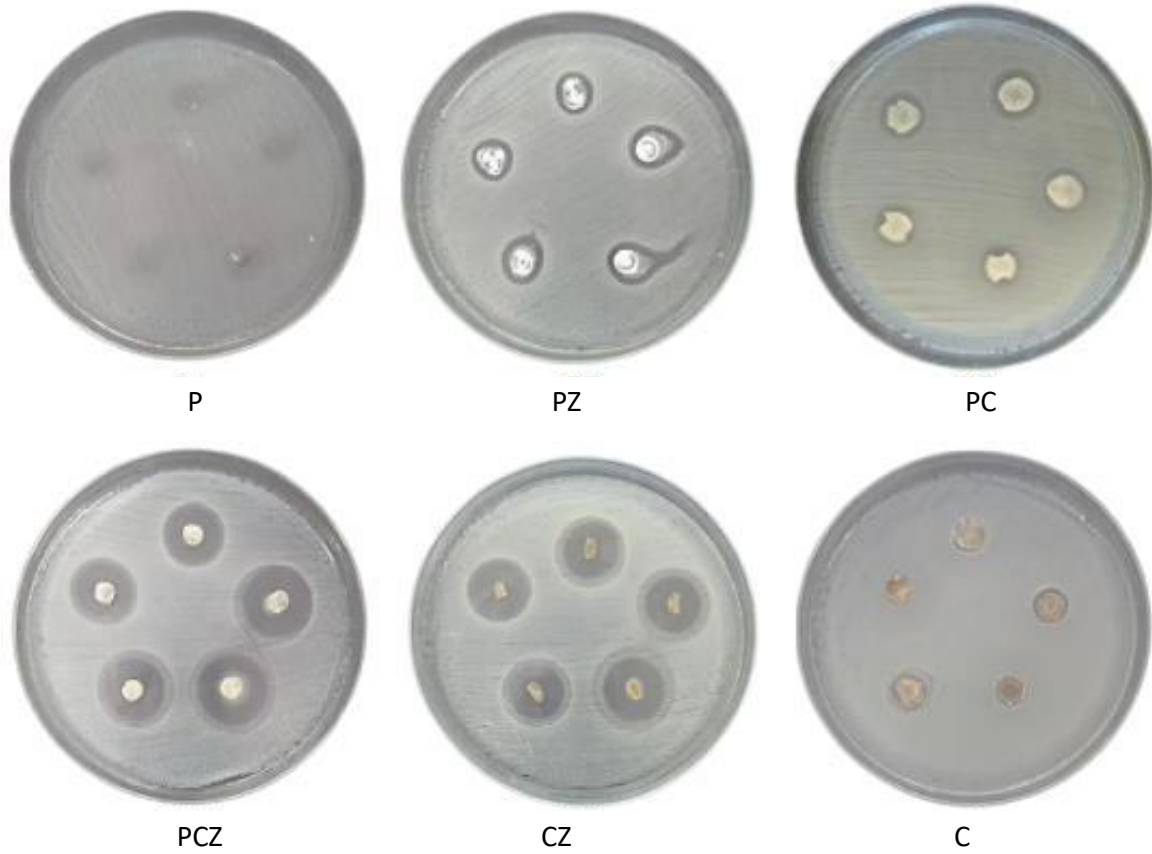
Source: Authors.

3.3 Antibacterial activity

The antibacterial activity of membranes against *S. aureus* was first evaluated by inhibition halo assays, which can be considered an adequate tool to evaluate the diffusive activity of compounds in the membranes as isolated and combined species. As shown in Figure 5, for experiments carried out in quintuplicate, the PVA membrane returned negligible antibacterial activity against *S. aureus*, as expected. The incorporation of zinc oxide into PVA (sample PZ) results in a discrete inhibition halo due to the eventual aggregation of nanoparticles. Intermediate values for inhibition haloes are observed for samples of PVA impregnated with chitosan (sample PC) – with a disadvantage relative to the high swelling ratio and the characteristic liquid uptake (see Figs. 4a and 4b) in response to the combination of the high hydrophilic behavior of both components as observed from experiments of swelling/ liquid uptake.

On the other hand, the best results (higher values for inhibitory haloes) are observed for samples CZ with an inhibition halo in order of 23.5 mm while for sample PCZ the value for inhibition halo is 26.3 mm, which is established as a result of the interaction of zinc oxide and chitosan. The characteristic high swelling ratio of the pure chitosan membrane was also observed in Figure 5 (sample C), revealing an apparent lower inhibition zone (in order of 12 mm) due to the variation in the chitosan disk dimensions as a result of the contact with the medium.

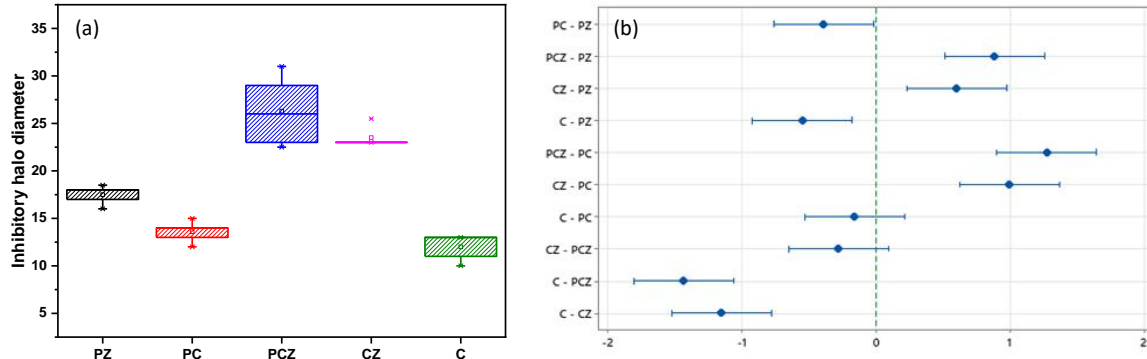
Figure 5 - Comparison of the inhibition haloes (performed in quintuplicate) for membranes with different compositions: P, PZ, PC, PCZ, CZ, and C in plates containing cultures of *S. aureus* after interaction with membranes. The incorporation of component C (chitosan) reinforces the antibacterial activity of the compound.



Source: Authors.

Results of means and standard deviation for inhibition haloes are summarized in Figure 6a in which is possible to confirm the higher values for inhibition haloes in PCZ-based membranes following the order $PCZ > CZ > PZ > PC > C$, in an indication that incorporation of zinc oxide and the combination with chitosan are relevant to reach superior performance in terms of the inhibition halo.

Figure 6 - (a) The plot of the inhibitory halo diameter and corresponding standard deviation as a function of the type of membrane (C, CZ, PC, PCZ and PZ) and (b) The plot of the confidence intervals for differences between means of halo diameters with a confidence of 95%.



Source: Authors.

The statistical significance of data in Figure 6a was determined by the p-value that was calculated to assess the hypothesis which claims the inhibitory halo diameter means are all equal to the results of the analysis of variance (see Table 1). As the $p\text{-value} \leq 0.05$, at least one statistically significant difference is established between the response of the membranes (the null hypothesis was rejected). In addition, a determination coefficient of 90.86% and a standard deviation of 0.196 were observed, indicating that the statistical model explains the variation observed for different inhibition zones obtained in analyzed membranes.

Table 1 - The one-way ANOVA table of the Completely Randomized Design (CRD).

SOURCE OF VARIATION	DF	SUM SQ	MEAN SQ	F-VALUE	P-VALUE
Sample	4	765.34	191.34	49.697	4.109×10^{-10}
Residuals	20	77.00	3.85		
Total	24	842.34			

Source: Authors.

Assuming that at least one significant sample is present in the group of the prepared membranes, the comparison of the means of the inhibition haloes of the groups was provided by Tukey's test. As shown by the Tukey grouping (summarized in Table 2 and Figure 6b) the confidence intervals of the difference between the mean responses of the samples revealed that only the pairs of the PCZ/CZ and PC/C groups showed no significant differences. This result reveals that the PVA has a negligible effect on the halo diameters, although the presence of the polymer in the membrane composition introduces a critical role in the retention of the properties of the resulting membranes (lower swelling rate).

Table 2 - Results of Tukey's test applied in the inhibition halo assays for different membranes (PCZ, CZ, PZ, PC and C) in terms of the means/ standard deviation and the corresponding Tukey grouping, confirming pairs (PCZ/CZ and PC/C).

SAMPLE	REPEATS	MEAN (MM)	STANDARD DEVIATION	TUKEY GROUPING
PCZ	5	26.3	2.960	A
CZ	5	23.5	0.800	A
PZ	5	17.5	0.800	B
PC	5	13.6	0.880	C
C	5	12.0	1.200	C

Source: Authors.

The results also show that there is a statistically significant difference between samples prepared with the combination of chitosan and zinc oxide in comparison with samples prepared in the presence of isolated components (chitosan or zinc oxide), confirming that the mutual incorporation of chitosan and zinc oxide can be considered an important condition to reach the maximum in the diffusion of the ROS components in the agar and that interaction of ZnO and chitosan introduces promising synergistic effects on the overall antibacterial activity of the material.

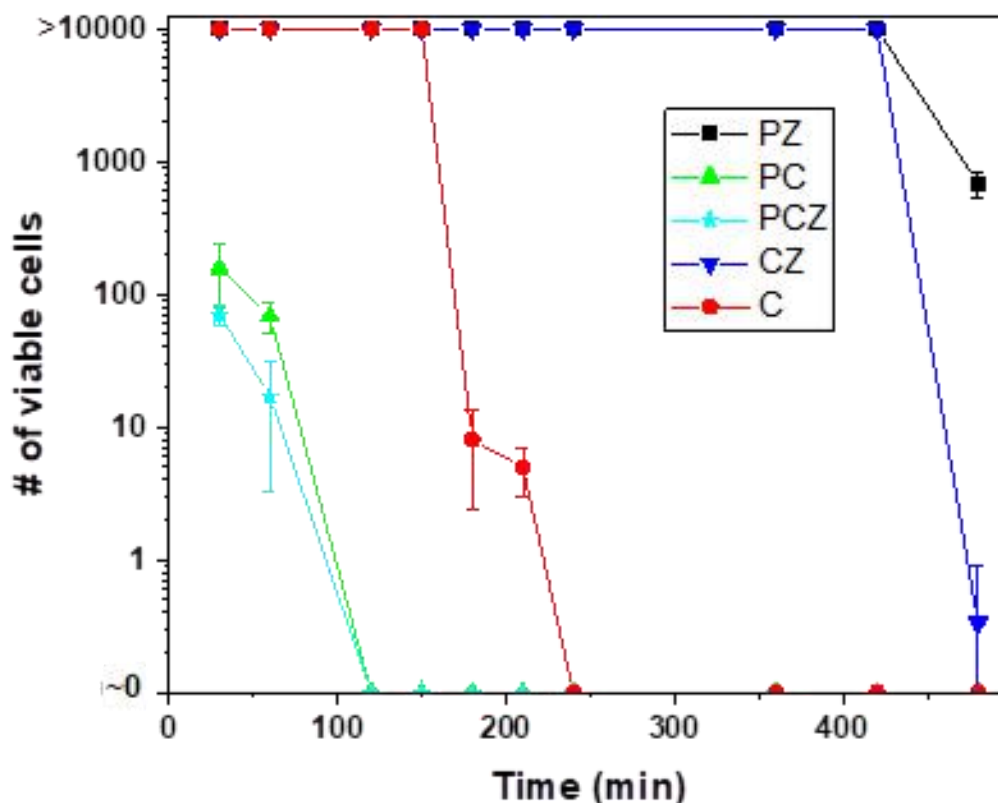
As reported in the literature, the antibacterial properties of chitosan are mainly due to the positive charge of its amine group, which reacts with the bacterial membrane affecting its permeability and inhibiting its growth (Hemmati et al., 2020; Sahariah et al., 2014). Relative to zinc oxide, it is worth mentioning that metal oxides are effective components against bacteria. However, in absence of a proper polymeric template or chelating agent, the components tend to agglomerate, reducing their antibacterial activity and effectiveness (Abureesh et al., 2018). Therefore, the use of a stabilizing agent has been necessary to prevent the coalescence of thermodynamically unstable nanoparticles in an aqueous medium (Rac-Rumijowska et al., 2017). The improvement in the antibacterial activity observed from the association of zinc oxide and chitosan can be considered a consequence of the reduction in the aggregation level of zinc oxide due to the dispersion of nanostructures in chitosan and the subsequent reduction in the hydrophilic behavior of chitosan with the dispersion of zinc oxide into the polymeric matrix. The superior performance of PVA-based membranes makes use of an additional component (polymeric matrix) that reduces the zinc oxide aggregation degree. On the other hand, the interaction of the polymeric template with zinc oxide restricts the strong mutual swelling of chitosan and PVA in an aqueous medium (Abdeen et al., 2018).

In addition to the inhibition halo assays, the kinetics of reduction in the number of viable bacterial cells (kill time assays) was determined from the counting of viable bacterial cells after a fixed exposure time of bacteria to solid membranes. Results summarized in Figure 7 indicate that a characteristic time interval of 420 min is required to observe a slight variation in the bacterial counting of the membranes composed of PZ and CZ. Intermediate performance is observed for membranes prepared with chitosan (complete elimination of bacteria after 240 min of treatment) while the best performance (faster removal of viable bacterial cells) was observed for samples PC and PCZ with the complete elimination of viable bacterial cells after 120 min of treatment, with the indication of fast kinetics for the antibacterial activity at the beginning of the reaction (less than 100 viable bacterial cells are present in the medium after 15 minutes of treatment), confirming the information provided by the inhibitory halo assays (strong antibacterial activity).

As reported in the literature, the presence of PVA can increase the mobility of cations as much as avoid unwanted agglomerations of metal oxides (Ciciliati et al., 2015), which degrade the antimicrobial activity of these oxides (Abureesh et al., 2018) while chitosan is reported to be a metal ion chelating agent (Ngah et al., 2011). Being assumed that Zn²⁺ chelation improves the biocompatibility of the chitosan-ZnO complex in comparison with the pure oxide (Zhong et al., 2018; Perelshtein et al., 2013). As a consequence, the incorporation of PVA in the membrane improves not only the retention of components for

a sustainable activity but also provides active sites (due to the homogeneous dispersion of components) for reactions of chelation of zinc by chitosan that potentialize the antibacterial activity of diffusive species.

Figure 7 - Dependence of the number of viable cells as a function of treatment time of membranes (PZ, PC, PCZ, CZ and C) – kill time kinetics against *S. aureus*.



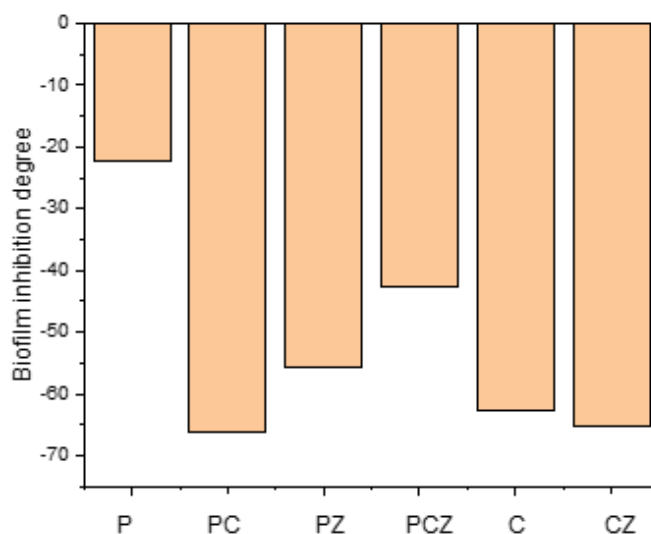
Source: Authors.

In addition to the diffusion of components and the kinetics of the antibacterial activity, the inhibition in the biofilm formation represents another important characteristic required for membranes with application in smart wound dressings. The measurement of biofilm inhibition was provided from a comparative experiment between biofilm formation on reactors (negative control) and the action of the corresponding systems with membranes applied as templates for the bacterial capture – the positive charge of chitosan, as an example, can be strongly explored for this purpose.

Due to the adhesion of crystal violet on biofilms, the intensity of absorbance at 570 nm provides an estimate of the concentration of adhered biofilms. Based on this aspect, the relative variation in the intensity of absorbance at characteristic peaks can be considered in the measurement of the antibiofilm activity of each material.

Figure 8 summarizes the relative variation in the absorbance at 570 nm (in %) for samples treated with different membranes and the negative control. As can be seen, pure PVA reduces the biofilm formation by 22.3% while stronger inhibitory activity is observed for samples prepared in the presence of chitosan, following the order PC>CZ>C>PZ>PCZ. The good performance in antibiofilm activity is observed for samples prepared in the presence of chitosan, as evidence that the positive net charge introduces electrostatic interaction activity with negatively charged bacterial cells in biofilms, that are attracted to the membrane surface, improving the antibiofilm activity of the resulting material.

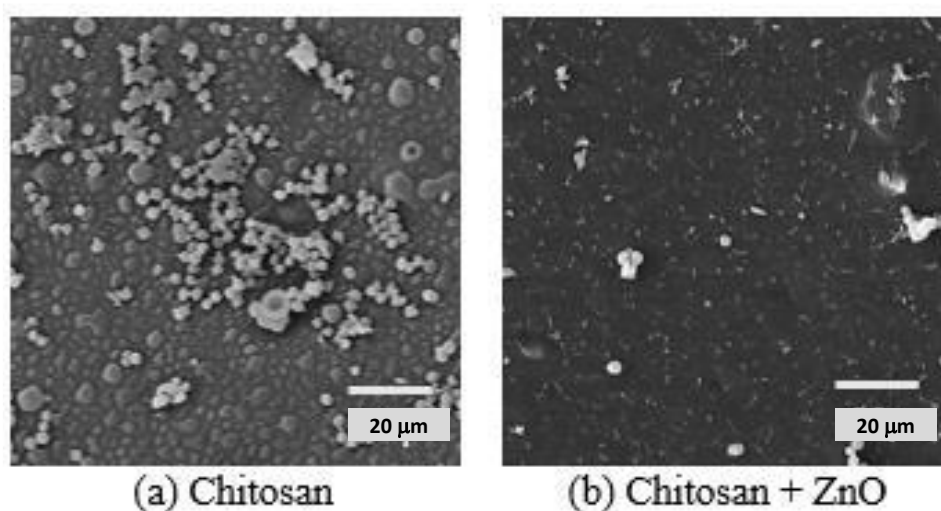
Figure 8 - Relative variation in the absorbance of stained bacterial cells for experimental systems treated with different membranes (P, PC, PZ, PCZ, C and CZ) in comparison with the control experiments (absence of antibacterial membranes)



Source: Authors.

These results are in agreement with data reported in the literature in which a strong reduction in the biofilm formation of *S. aureus* is observed with values of 67% for chitosan-zinc oxide nanocomposites (Hemmati et al., 2020). SEM images (shown in Figure 9) for samples C and CZ confirm the adhesion degree of bacterial cells on the membranes' surface. There are a few bacterial cells and a high number of lysed cells on the chitosan membrane whereas few traces of bacteria can be found on the chitosan-ZnO composite. It is worth mentioning that the presence of PVA favors the dissolution of the membrane after continuous stirring in the biofilm formation assay due to the hydrophilic nature of the polymer (after 24 h of contact with an aqueous solution).

Figure 9 - Comparison of the membrane surfaces after contact with *S. aureus* for samples (a) chitosan and (b) chitosan+ZnO.



Source: Authors.

The reduction in the biofilm formation has been attributed to the creation of several water channels in the biofilm that facilitates the migration of nanoparticles, the diffusion of the reactive species along with pores of bacteria (explored for

transportation of nutrients), and the inhibition of efflux pump processes. The strong interaction of zinc oxide and chitosan immersed in a PVA matrix returned a lower performance in comparison with PC and CZ due to the restrictions in the volume variation due to the mutual interaction of the three components. The use of a combinatory antibiofilm strategy in *S. aureus* may be better to maintain the balance of microbiota and to perform a better control of microbial infections (bacterial and viral) in comparison with monotherapy (Wang et al., 2018). As a consequence, the reduction in the swelling of the membrane reduces the effective area for biofilm removal from reactors. On the other hand, the preserved structure of the membrane favors the complete removal of the material after treatment (an advantage for chitosan-based membranes).

Based on these aspects, it is possible to observe that the reported properties of the complex of chitosan and zinc oxide (in terms of diffusion of reactive species and fast kinetics of antibacterial activity) can be conveniently explored in the presence of a polymeric template of PVA. The association of components in PCZ membranes circumvents typical drawbacks related to swelling of PC and C membranes, introducing an additional advantage for the removal of the membrane after treatment (for the prototype of wound dressing systems) and the minimal aggregation of the active antibacterial agents.

4. Conclusion

The good performance observed for mixed compounds of PVA/ZnO/chitosan in terms of the diffusion of species, kill time and antibiofilm activity is a result of the effects of positive net charge of chitosan and its chelating behavior in association with the production of Zn^{2+} ions and reactive species that makes use of the retention in the swelling ratio provided by the PVA. The combined activity of the PCZ sample returned important results for the fast kinetics of the bacterial kill time and a strong reduction in the viable bacterial cells from 106 CFU to 102 CFU after 15 min of treatment, confirming the promising application of membranes against bacterial proliferation and biofilm formation with the reduction in the order of 67% for sample PC with the improved antibiofilm activity assigned to the cationic charge of the chitosan-based membranes.

Acknowledgments

This work was supported by Brazilian funding agencies, FINEP, FACEPE (APQ-0444-1.05/20), CNPq, and Coordenação de Aperfeiçoamento de Pessoal de Nível Superior – Brazil (CAPES) – Finance Code 001.

References

- Abdeen, Z. I., El Faragy, A. F., & Negm, N. A. (2018). Nanocomposite framework of chitosan/polyvinyl alcohol/ZnO: Preparation, characterization, swelling and antimicrobial evaluation. *Journal of Molecular Liquids*, 250, 335–343. <https://doi.org/https://doi.org/10.1016/j.molliq.2017.12.032>
- Abureesh, M. A., Oladipo, A. A., Mizwari, Z. M., & Berksel, E. (2018). Engineered mixed oxide-based polymeric composites for enhanced antimicrobial activity and sustained release of antiretroviral drug. *International Journal of Biological Macromolecules*, 116, 417–425. <https://doi.org/10.1016/J.IJBIOMAC.2018.05.065>
- Ahmad Yusof, N. A., Mat Zain, N., & Pauzi, N. (2019). Synthesis of Chitosan/Zinc Oxide Nanoparticles Stabilized by Chitosan via Microwave Heating. *Bulletin of Chemical Reaction Engineering & Catalysis*, 14(2), 450. <https://doi.org/10.9767/bcrec.14.2.3319.450-458>
- Aslam, M., Kalyar, M. A., & Raza, Z. A. (2018). Investigation of Zinc Oxide-Loaded Poly(Vinyl Alcohol) Nanocomposite Films in Tailoring Their Structural, Optical and Mechanical Properties. *Journal of Electronic Materials*, 47(7), 3912–3926. <https://doi.org/10.1007/s11664-018-6270-1>
- Aslam, M., Kalyar, M. A., & Raza, Z. A. (2019). Effect of Separate Zinc, Copper and Graphene Oxides Nanofillers on Electrical Properties of PVA Based Composite Strips. *Journal of Electronic Materials*, 48(2), 1116–1121. <https://doi.org/10.1007/s11664-018-6793-5>
- Aslam, M., Kalyar, M. A., & Raza, Z. A. (2021). Fabrication of nano-CuO-loaded PVA composite films with enhanced optomechanical properties. *Polymer Bulletin*, 78(3), 1551–1571. <https://doi.org/10.1007/s00289-020-03173-9>
- Aslam, M., Raza, Z. A., & Siddique, A. (2021). Fabrication and chemo-physical characterization of CuO/chitosan nanocomposite-mediated tricomponent PVA films. *Polymer Bulletin*, 78(4), 1955–1965. <https://doi.org/10.1007/s00289-020-03194-4>
- Ayub, A., & Raza, Z. A. (2021). Arsenic removal approaches: A focus on chitosan biosorption to conserve the water sources. *International Journal of Biological Macromolecules*, 192, 1196–1216. <https://doi.org/https://doi.org/10.1016/j.ijbiomac.2021.10.050>

- Ayub, A., Raza, Z. A., Majeed, M. I., Tariq, M. R., & Irfan, A. (2020). Development of sustainable magnetic chitosan biosorbent beads for kinetic remediation of arsenic contaminated water. *International Journal of Biological Macromolecules*, 163, 603–617. <https://doi.org/https://doi.org/10.1016/j.ijbiomac.2020.06.287>
- Barreto, M. S. R., Andrade, C. T., Azero, E. G., Paschoalin, V. M. F., & Del Aguila, E. M. (2017). Production of chitosan/zinc oxide complex by ultrasonic treatment with antibacterial activity. *Journal of Bacteriology & Parasitology*, 8(5), 1–7. <https://doi.org/10.4172/2155-9597.1000330>
- Bhattacharjee, B., Ghosh, S., Mukherjee, R., & Haldar, J. (2021). Quaternary lipophilic chitosan and gelatin cross-linked antibacterial hydrogel effectively kills multidrug-resistant bacteria with minimal toxicity toward mammalian cells. *Biomacromolecules*, 22(2), 557–571. <https://doi.org/10.1021/acs.biomac.0c01420>
- Bhattacharya, M., Wozniak, D. J., Stoodley, P., & Hall-Stoodley, L. (2015). Prevention and treatment of *Staphylococcus aureus* biofilms. *Expert Review of Anti-Infective Therapy*, 13(12), 1499–1516. <https://doi.org/10.1586/14787210.2015.1100533>
- Bobu, E., Nicu, R., Lupei, M., Ciolacu, F., & Desbrieres, J. (2011). Synthesis and characterization of n-alkyl chitosan for papermaking applications. *Cellulose Chemistry and Technology*, 45, 619–625.
- Brandt, S. L., Putnam, N. E., Cassat, J. E., & Serezani, C. H. (2018). Innate immunity to *Staphylococcus aureus*: Evolving paradigms in soft tissue and invasive infections. *The Journal of Immunology*, 200(12), 3871–3880. <https://doi.org/10.4049/jimmunol.1701574>
- Burnham, J. P., & Kollef, M. H. (2018). Treatment of severe skin and soft tissue infections: A review. *Current Opinion in Infectious Diseases*, 31(2), 113–119. <https://doi.org/10.1097/QCO.0000000000000431>
- Ciciliati, M. A., Silva, M. F., Fernandes, D. M., Melo, M. A. C., Hechenleitner, A. A. W., & Pineda, E. A. G. (2015). Fe-doped ZnO nanoparticles: synthesis by a modified sol–gel method and characterization. *Materials Letters*, 159, 84–86. <https://doi.org/10.1016/J.MATLET.2015.06.023>
- Cuero, R. G., Osuji, G., & Washington, A. (1991). N-carboxymethylchitosan inhibition of aflatoxin production: Role of zinc. *Biotechnology Letters*, 13(6), 441–444. <https://doi.org/10.1007/BF01030998>
- Dadi, R., Azouani, R., Traore, M., Mielcarek, C., & Kanaev, A. (2019). Antibacterial activity of ZnO and CuO nanoparticles against gram positive and gram negative strains. *Materials Science and Engineering C*, 104, 109968. <https://doi.org/10.1016/j.msec.2019.109968>
- Delgadillo-Armendariz, N. L., Rangel-Vazquez, N. A., Marquez-Brazon, E. A., & Gascue, B. R.-D. (2014). Interactions of chitosan/genipin hydrogels during drug delivery: A QSPR APPROACH. *Química Nova*, 37, 1503–1509. <https://doi.org/10.5935/0100-4042.20140243>
- Dharmaraj, D., Krishnamoorthy, M., Rajendran, K., Karupiah, K., Annamalai, J., Durairaj, K. R., Santhiyagu, P., & Ethiraj, K. (2021). Antibacterial and cytotoxicity activities of biosynthesized silver oxide (Ag₂O) nanoparticles using *Bacillus paramycoides*. *Journal of Drug Delivery Science and Technology*, 61, 102111. <https://doi.org/10.1016/j.jddst.2020.102111>
- Djurišić, A. B., Leung, Y. H., Ng, A. M. C., Xu, X. Y., Lee, P. K. H., Degger, N., & Wu, R. S. S. (2015). Toxicity of metal oxide nanoparticles: Mechanisms, characterization, and avoiding experimental artefacts. *Small*, 11(1), 26–44. <https://doi.org/10.1002/sml.201303947>
- Fahmy, A., Kamoun, E. A., El-Eisawy, R., El-Fakharany, E. M., Taha, T. H., El-Damhougy, B. K., & Abdelhai, F. (2015). Poly(vinyl alcohol)-hyaluronic Acid Membranes for Wound Dressing Applications: Synthesis and in vitro Bio-Evaluations. *Journal of the Brazilian Chemical Society*, 26, 1466–1474. <https://doi.org/10.5935/0103-5053.20150115>
- Feng, B.-H., & Peng, L.-F. (2012). Synthesis and characterization of carboxymethyl chitosan carrying ricinoleic functions as an emulsifier for azadirachtin. *Carbohydrate Polymers*, 88(2), 576–582. <https://doi.org/https://doi.org/10.1016/j.carbpol.2012.01.002>
- Gavalyan, V. B. (2016). Synthesis and characterization of new chitosan-based Schiff base compounds. *Carbohydrate Polymers*, 145, 37–47. <https://doi.org/https://doi.org/10.1016/j.carbpol.2016.02.076>
- Godoy-Gallardo, M., Eckhard, U., Delgado, L. M., Puente, Y. J. D. R., Hoyos-Nogués, M., Gil, F. J., & Perez, R. A. (2021). Antibacterial approaches in tissue engineering using metal ions and nanoparticles: from mechanisms to applications. *Bioactive Materials*, 6(12), 4470–4490. <https://doi.org/10.1016/j.bioactmat.2021.04.033>
- Gudkov, S. V., Burmistrov, D. E., Serov, D. A., Rebezov, M. B., Semenova, A. A., & Lisitsyn, A. B. (2021). A Mini Review of Antibacterial Properties of ZnO Nanoparticles. *Frontiers in Physics*, 9, 641181. <https://doi.org/10.3389/fphy.2021.641181>
- Hajizadeh, H., Peighambaroust, S. J., Peighambaroust, S. H., & Peressini, D. (2020). Physical, mechanical, and antibacterial characteristics of bio-nanocomposite films loaded with Ag-modified SiO₂ and TiO₂ nanoparticles. *Journal of Food Science*, 85(4), 1193–1202. <https://doi.org/10.1111/1750-3841.15079>
- Hemmati, F., Salehi, R., Ghotaslou, R., Kafil, H. S., Hasani, A., Gholizadeh, P., & Rezaee, M. A. (2020). The assessment of antibiofilm activity of chitosan-zinc oxide-gentamicin nanocomposite on *Pseudomonas aeruginosa* and *Staphylococcus aureus*. *International Journal of Biological Macromolecules*, 163, 2248–2258. <https://doi.org/10.1016/J.IJBIOMAC.2020.09.037>
- Inbaraj, B. S., Chen, B. Y., Liao, C. W., & Chen, B. H. (2020). Green synthesis, characterization and evaluation of catalytic and antibacterial activities of chitosan, glycol chitosan and poly(γ -glutamic acid) capped gold nanoparticles. *International Journal of Biological Macromolecules*, 161, 1484–1495. <https://doi.org/10.1016/j.ijbiomac.2020.07.244>
- Jiang, J., Pi, J., & Cai, J. (2018). The advancing of zinc oxide nanoparticles for biomedical applications. *Bioinorganic Chemistry and Applications*, 2018, 1062562. <https://doi.org/10.1155/2018/1062562>
- Kadiyala, U., Turali-Emre, E. S., Bahng, J. H., Kotov, N. A., Scott Vanepps, J., & VanEpps, J. S. (2018). Unexpected insights into antibacterial activity of zinc oxide nanoparticles against methicillin resistant: *Staphylococcus aureus* (MRSA). *Nanoscale*, 10(10), 4927–4939. <https://doi.org/10.1039/c7nr08499d>

- Kajbafvala, A., Zanganeh, S., Kajbafvala, E., Zargar, H. R., Bayati, M. R., & Sadmezhaad, S. K. (2010). Microwave-assisted synthesis of narciss-like zinc oxide nanostructures. *Journal of Alloys and Compounds*, 497(1–2), 325–329. <https://doi.org/10.1016/J.JALLCOM.2010.03.057>
- Kamoun, E. A., Kenawy, E.-R. S., Tamer, T. M., El-Meligy, M. A., & Mohy Eldin, M. S. (2015). Poly (vinyl alcohol)-alginate physically crosslinked hydrogel membranes for wound dressing applications: Characterization and bio-evaluation. *Arabian Journal of Chemistry*, 8(1), 38–47. <https://doi.org/https://doi.org/10.1016/j.arabjc.2013.12.003>
- Karthikeyan, C., Varaprasad, K., Akbari-Fakhrabadi, A., Hameed, A. S. H., & Sadiku, R. (2020). Biomolecule chitosan, curcumin and ZnO-based antibacterial nanomaterial, via a one-pot process. *Carbohydrate Polymers*, 249, 116825. <https://doi.org/https://doi.org/10.1016/j.carbpol.2020.116825>
- Khalilipour, A., & Paydayesh, A. (2019). Characterization of Polyvinyl Alcohol/ZnO Nanocomposite Hydrogels for Wound Dressings. *Journal of Macromolecular Science, Part B*, 58(2), 371–384. <https://doi.org/10.1080/00222348.2018.1560936>
- Khan, M. F., Ansari, A. H., Hameedullah, M., Ahmad, E., Husain, F. M., Zia, Q., Baig, U., Zaheer, M. R., Alam, M. M., Khan, A. M., AlOthman, Z. A., Ahmad, I., Ashraf, G. M., & Aliev, G. (2016). Sol-gel synthesis of thorn-like ZnO nanoparticles endorsing mechanical stirring effect and their antimicrobial activities: Potential role as nano-antibiotics. *Scientific Reports*, 6(1), 27689. <https://doi.org/10.1038/srep27689>
- Kotov, N. A. (2010). Inorganic nanoparticles as protein mimics. *Science*, 330(6001), 188–189. <https://doi.org/10.1126/science.1190094>
- Krishnaveni, R., & Thambidurai, S. (2013). Industrial method of cotton fabric finishing with chitosan-ZnO composite for anti-bacterial and thermal stability. *Industrial Crops and Products*, 47, 160–167. <https://doi.org/10.1016/j.indcrop.2013.03.007>
- Lemire, J. A., Harrison, J. J., & Turner, R. J. (2013). Antimicrobial activity of metals: Mechanisms, molecular targets and applications. *Nature Reviews Microbiology*, 11(6), 371–384. <https://doi.org/10.1038/nrmicro3028>
- Li, L.-H., Deng, J.-C., Deng, H.-R., Liu, Z.-L., & Xin, L. (2010). Synthesis and characterization of chitosan/ZnO nanoparticle composite membranes. *Carbohydrate Research*, 345(8), 994–998. <https://doi.org/https://doi.org/10.1016/j.carres.2010.03.019>
- Ma, Z., Garrido-Maestu, A., & Jeong, K. C. (2017). Application, mode of action, and in vivo activity of chitosan and its micro- and nanoparticles as antimicrobial agents: A review. *Carbohydrate Polymers*, 176, 257–265. <https://doi.org/10.1016/j.carbpol.2017.08.082>
- Maji, J., Pandey, S., & Basu, S. (2020). Synthesis and evaluation of antibacterial properties of magnesium oxide nanoparticles. *Bulletin of Materials Science*, 43(1), 1–10. <https://doi.org/10.1007/s12034-019-1963-5>
- McDevitt, C. A., Ogunniyi, A. D., Valkov, E., Lawrence, M. C., Kobe, B., McEwan, A. G., & Paton, J. C. (2011). A Molecular Mechanism for Bacterial Susceptibility to Zinc. *PLOS Pathogens*, 7(11), e1002357.
- Milonis, A., Tripathy, A., Donati, M., Sharma, C. S., Pan, F., Maniura-Weber, K., Ren, Q., & Poulidakos, D. (2020). Water-Based Scalable Methods for Self-Cleaning Antibacterial ZnO-Nanostructured Surfaces. *Industrial and Engineering Chemistry Research*, 59(32), 14323–14333. <https://doi.org/10.1021/acs.iecr.0c01998>
- Moeini, A., Pedram, P., Makvandi, P., Malinconico, M., & D'Ayala, G. G. (2020). Wound healing and antimicrobial effect of active secondary metabolites in chitosan-based wound dressings: A review. *Carbohydrate Polymers*, 233, 115839. <https://doi.org/10.1016/j.carbpol.2020.115839>
- Mushtaq, F., Nazeer, M. A., Mansha, A., Zahid, M., Bhatti, H. N., Raza, Z. A., Yaseen, W., Rafique, A., & Irshad, R. (2022). Poly(Vinyl Alcohol) (PVA)-Based Treatment Technologies in the Remediation of Dye-Containing Textile Wastewater BT - Polymer Technology in Dye-containing Wastewater: Volume 2 (A. Khadir & S. S. Muthu, Eds.; pp. 1–21). Springer Nature Singapore. https://doi.org/10.1007/978-981-19-0886-6_1
- Nasu, A., & Otsubo, Y. (2006). Rheology and UV protection properties of suspensions of fine titanium dioxides in a silicone oil. *Journal of Colloid and Interface Science*, 296(2), 558–564. <https://doi.org/10.1016/j.jcis.2005.09.036>
- Ngah, W. S. W., Teong, L. C., & Hanafiah, M. A. K. M. (2011). Adsorption of dyes and heavy metal ions by chitosan composites: a review. *Carbohydrate Polymers*, 83(4), 1446–1456. <https://doi.org/10.1016/J.CARBPOL.2010.11.004>
- Niño-Martínez, N., Oroco, M. F. S., Martínez-Castañón, G. A., Méndez, F. T., & Ruiz, F. (2019). Molecular mechanisms of bacterial resistance to metal and metal oxide nanoparticles. *International Journal of Molecular Sciences*, 20(11), 2808. <https://doi.org/10.3390/ijms20112808>
- Paul, S., Jayan, A., Sasikumar, C. S., & Cherian, S. M. (2014). Extraction and Purification of Chitosan from Chitin Isolated from Sea Prawn (*Fenneropenaeus indicus*). *Asian Journal of Pharmaceutical and Clinical Research*, 7(4), 201–204.
- Perelshtein, I., Ruderman, E., Perkash, N., Tzanov, T., Beddow, J., Joyce, E., Mason, T. J., Blanes, M., Mollá, K., Patlolla, A., Frenkel, A. I., & Gedanken, A. (2013). Chitosan and chitosan-ZnO-based complex nanoparticles: formation, characterization, and antibacterial activity. *Journal of Materials Chemistry B*, 1(14), 1968–1976. <https://doi.org/10.1039/C3TB00555K>
- Qi, K., Cheng, B., Yu, J., & Ho, W. (2017). Review on the improvement of the photocatalytic and antibacterial activities of ZnO. *Journal of Alloys and Compounds*, 727, 792–820. <https://doi.org/10.1016/j.jallcom.2017.08.142>
- Rac-Rumijowska, O., Fiedot, M., Suchorska-Wozniak, P., & Teterycz, H. (2017). Synthesis of gold nanoparticles with different kinds of stabilizing agents. Proceedings of the International Spring Seminar on Electronics Technology, 2017, 1–6. <https://doi.org/10.1109/ISSE.2017.8000972>
- Raza, Z. A., Khalil, S., Ayub, A., & Banat, I. M. (2020). Recent developments in chitosan encapsulation of various active ingredients for multifunctional applications. *Carbohydrate Research*, 492, 108004. <https://doi.org/https://doi.org/10.1016/j.carres.2020.108004>
- Reddy, K. M., Feris, K., Bell, J., Wingett, D. G., Hanley, C., & Punnoose, A. (2007). Selective toxicity of zinc oxide nanoparticles to prokaryotic and eukaryotic systems. *Applied Physics Letters*, 90(213902), 2139021–2139023. <https://doi.org/10.1063/1.2742324>

Sahariah, P., Gaware, V. S., Lieder, R., Jónsdóttir, S., Hjálmarsdóttir, M. A., Sigurjonsson, O. E., & Másson, M. (2014). The effect of substituent, degree of acetylation and positioning of the cationic charge on the antibacterial activity of quaternary chitosan derivatives. *Marine Drugs*, 12(8), 4635–4658. <https://doi.org/10.3390/MD12084635>

Singh, P., Kumar, R., & Singh, R. K. (2019). Progress on Transition Metal-Doped ZnO Nanoparticles and Its Application. *Industrial and Engineering Chemistry Research*, 58(37), 17130–17163. <https://doi.org/10.1021/acs.iecr.9b01561>

Soren, S., Kumar, S., Mishra, S., Jena, P. K., Verma, S. K., & Parhi, P. (2018). Evaluation of antibacterial and antioxidant potential of the zinc oxide nanoparticles synthesized by aqueous and polyol method. *Microbial Pathogenesis*, 119, 145–151.

Souza, R. C., Haberbeck, L. U., Riella, H. G., Ribeiro, D. H. B., & Carciofi, B. A. M. (2019). Antibacterial activity of zinc oxide nanoparticles synthesized by solochemical process. *Brazilian Journal of Chemical Engineering*, 36(2), 885–893. <https://doi.org/10.1590/0104-6632.20190362S20180027>

Wang, Y., Tan, X., Xi, C., & Phillips, K. S. (2018). Removal of *Staphylococcus aureus* from skin using a combination antibiofilm approach. *Npj Biofilms and Microbiomes*, 4(1), 16. <https://doi.org/10.1038/s41522-018-0060-7>

Xia, J., Zhang, H., Yu, F., Pei, Y., & Luo, X. (2020). Superclear, Porous Cellulose Membranes with Chitosan-Coated Nanofibers for Visualized Cutaneous Wound Healing Dressing. *ACS Applied Materials and Interfaces*, 12(21), 24370–24379. <https://doi.org/10.1021/acsami.0c05604>

Zhong, Q., Tian, J., Liu, T., Guo, Z., Ding, S., & Li, H. (2018). Preparation and antibacterial properties of carboxymethyl chitosan/ZnO nanocomposite microspheres with enhanced biocompatibility. *Materials Letters*, 212, 58–61. <https://doi.org/10.1016/J.MATLET.2017.10.062>